



HAL
open science

Modelling Dynamic Conformations of Organic Molecules: Alkyne Carotenoids in Solution

Simona Streckaitė, Mindaugas Macernis, Fei Li, Eliška Kuthanová Trsková, Radek Litvin, Chunhong Yang, Andrew A. Pascal, Leonas Valkunas, Bruno Robert, Manuel J. Llansola-Portoles

► **To cite this version:**

Simona Streckaitė, Mindaugas Macernis, Fei Li, Eliška Kuthanová Trsková, Radek Litvin, et al.. Modelling Dynamic Conformations of Organic Molecules: Alkyne Carotenoids in Solution. *Journal of Physical Chemistry A*, 2020, 10.1021/acs.jpca.9b11536 . hal-02509022

HAL Id: hal-02509022

<https://hal.science/hal-02509022>

Submitted on 18 Nov 2020

HAL is a multi-disciplinary open access archive for the deposit and dissemination of scientific research documents, whether they are published or not. The documents may come from teaching and research institutions in France or abroad, or from public or private research centers.

L'archive ouverte pluridisciplinaire **HAL**, est destinée au dépôt et à la diffusion de documents scientifiques de niveau recherche, publiés ou non, émanant des établissements d'enseignement et de recherche français ou étrangers, des laboratoires publics ou privés.

Modelling Dynamic Conformations of Organic Molecules: Alkyne Carotenoids in Solution

Simona Streckaite^{a†}, Mindaugas Macernis^{b†}, Fei Li^{a,c}, Eliška Kuthanová Trsková^{d,e}, Radek Litvin^{d,e}, Chunhong Yang^c, Andrew A. Pascal^a, Leonas Valkunas^{b,g*}, Bruno Robert^{a*}, Manuel J. Llansola-Portoles^{a*}

- a) Université Paris-Saclay, CEA, CNRS, Institute for Integrative Biology of the Cell (I2BC), 91198, Gif-sur-Yvette, France
- b) Institute of Chemical Physics, Faculty of Physics, Vilnius University, Saulėtekio Ave. 3, LT-10222, Vilnius, Lithuania
- c) Key Laboratory of Photobiology, Institute of Botany, Chinese Academy of Sciences, Beijing 100093, People's Republic of China
- d) Biology Centre, Czech Academy of Sciences, Branisovska 31, 370 05 Ceske Budejovice, Czech Republic
- e) Faculty of Science, University of South Bohemia, Branisovska 1760, 370 05 Ceske Budejovice, Czech Republic
- f) Institute of Microbiology, Academy of Sciences of the Czech Republic, 379 81, Třeboň, Czech Republic
- g) Molecular Compounds Physics Department, Center for Physical Sciences and Technology, Sauletekio Ave. 3, LT-10257, Vilnius, Lithuania

[†]: equivalent authors

^{*}: corresponding authors

Leonas Valkunas; e-mail: leonas.valkunas@ff.vu.lt

Bruno Robert ; e-mail: Bruno.ROBERT@cea.fr

Manuel J. Llansola-Portoles ; e-mail: manuel.llansola@i2bc.paris-saclay.fr

Abstract

Calculating the spectroscopic properties of complex conjugated organic molecules in their relaxed state is far from simple. An additional complexity arises for flexible molecules in solution, where the rotational energy barriers are low enough so that non-minimum conformations may become dynamically populated. These metastable conformations quickly relax during the minimization procedures preliminary to DFT calculations, and so accounting for their contribution to the experimentally-observed properties is problematic. We describe a strategy for stabilising these non-minimum conformations *in silico*, allowing their properties to be calculated. Diadinoxanthin and alloxanthin present atypical vibrational properties in solution, indicating the presence of several conformations. Performing energy calculations *in vacuo* and polarizable continuum model calculations in different solvents, we found three different conformations with values for the δ dihedral angle of the end-ring ca. 0° , 180° and 90° with respect to the plane of the conjugated chain. The latter conformation, a non-global minimum, is not stable during the minimization necessary for modelling its spectroscopic properties. To circumvent this classical problem we used a Car-Parinello MD supermolecular approach, in which diadinoxanthin was solvated by water molecules so that metastable conformations were stabilized by hydrogen-bonding interactions. We progressively removed the number of solvating waters to find the minimum required for this stabilisation. This strategy represents the first modelling of a carotenoid in a distorted conformation, and provides an accurate interpretation of the experimental data.

Introduction

Modelling the vibrational and electronic properties of complex conjugated organic molecules has tremendously progressed in the last twenty years, due to the development of DFT and TD-DFT methods and their combination with QM/MM calculations or studies using *ab initio* molecular dynamics (QMD)¹⁻¹². It is now possible to get quite precise estimations of the electronic and vibrational properties of such molecules, and to disentangle the parameters able to tune these properties. However, for some molecules, the energy barriers to rotation around certain bonds are low enough so that non-minimum conformations become dynamically populated (in solution at room temperature, for instance). Calculating the molecular properties of these molecules using only their global energy minima may thus not fully account for the experimental observations. Similarly, it is often impossible to account for the properties of protein-bound molecules, when the binding site constrains them in a non-minimum conformation. Even though local minima can be predicted by theory, the vibrational and electronic properties of the molecules in such local minima cannot be precisely assessed - as these metastable conformations quickly relax to global minima during the energy optimization procedures defined by DFT calculations¹³⁻¹⁵. This constitutes a major challenge for accurately addressing the behaviour of non-rigid molecules by theoretical approaches. In this paper, we report a strategy to circumvent this obstacle, which in many cases is at the origin of deviations between theoretical predictions and experimental observations.

Built from the assembly of isoprenoid units, carotenoids are one of the most important families of conjugated molecules in Nature - being present in every biological kingdom. In photosynthetic organisms, carotenoids act both as light-harvesters and photoprotective molecules during the first steps of the photosynthetic process¹⁶⁻¹⁷. They represent an important player in complex biological signalling processes, as the colour of a wide range of organisms is carotenoid-based¹⁸⁻²². The origin of the functional properties of carotenoids directly correlates with their linear conjugated polyene chain. A model involving three low-energy excited states has been proposed in the literature to describe their electronic properties²³⁻²⁸. Carotenoid molecules generally exhibit strong electronic absorption, arising from a transition from the ground state to the second excited state ($S_0 \rightarrow S_2$); for simplicity, we will define this transition by the energy corresponding to the lowest vibronic sublevel (0-0). The first excited state exhibits the same symmetry as the ground state, and is thus optically silent (in one-photon absorption)²³. For linear carotenoids, the 0-0 transition energy tightly depends on the conjugation length²⁹⁻³⁰. Natural carotenoids display large structural diversity, as their carbon

skeletons may include several functional groups, which may be conjugated with the isoprenoid chain (including substituted cycles). The presence of such additional conjugated groups modifies the electronic properties of these molecules, and thus may tune their biological function¹⁶. In such cases, the vibrational and electronic properties can be related to an artificial parameter *effective conjugation length* (N_{eff}), defined as the number of conjugated carbon-carbon double bonds in linear carotenoids that would account for the vibrational and electronic properties of the complex carotenoid²⁹⁻³⁰.

Due to the isoprenoid structure, calculation of their full electronic structure and vibrational properties have proven complex even for the simplest carotenoid molecules. Considerable progress has been achieved in this field, and prediction of the electronic behaviour of non-distorted carotenoids has become feasible³¹. However, carotenoids often adopt distorted conformations when bound to proteins, corresponding to out-of-plane deviations of the molecule due to rotations around C-C single bonds of the isoprenoid chain. Their precise characterisation requires the analysis of their photochemistry in different solvents, which, as a basis, implicates a detailed characterisation of their conformation. For β -carotene in solvent, it was recently shown that the molecule displays out-of-plane deviations of its conjugated end-cycles, while in some proteins the conjugated end-cycles are constrained in the molecular plane, resulting in an increase of the effective conjugation length of the molecule³²⁻³³. In all these cases, theoretical modelling can only address the properties of these molecules in their global minima, so that an accurate account of the influence of these distortions is not currently possible.

Diadinoxanthin (Ddx) and alloxanthin (Allo), two complex carotenoids bearing alkyne groups within the linear conjugated chain (Figure 1), are employed by some photosynthetic organisms as light-harvesting and photoprotective pigments³⁴⁻³⁶. In this paper, we show that the properties of these carotenoids cannot be predicted by standard DFT-based approaches, due to the dynamic population of local minima. The introduction of solvent in the calculations has been shown to stabilize different minima³⁷, and so we tested a new strategy based on this stabilisation, to model the properties of organic molecules in metastable conformations corresponding to a local minimum. In this approach, we stabilize this conformation using water molecules and perform the calculation on the carotenoid/water ensemble. The results are compared with experimental data, and the importance of such sub-minimal conformers is discussed.

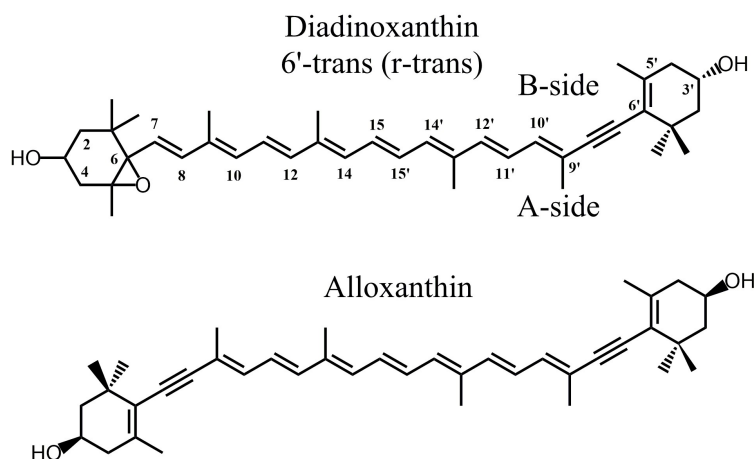


Figure 1/ Molecular structures of the carotenoids studied: diadinoxanthin and alloxanthin. The δ angle represents the dihedral angle between $C10'-C9'-C6'-C5'$, which characterises the rotation of the conjugated end-ring relative to the plane of the polyene chain.

Nomenclature

Ddx and Allo contain a conjugated cycle on one end (Ddx) or both (Allo), which may present isomerization around the carbon at position 6' (and 6). As such isomers are distinct from isomerization in the linear chain, we distinguish them by using the nomenclature *r-cis*, *r-trans* or *r-gauche* rather than the IUPAC 6'-*cis*, 6'-*trans* or 6'-*gauche*³⁸ - where «r-» stands for «isomerization of the end-ring relative to the linear backbone».

Experimental Results

Electronic and Vibrational Properties of Diadinoxanthin.

The nominal conjugation length of diadinoxanthin is 10 – eight C=C double bonds plus a triple bond (alkyne) in the linear chain, and one C=C in the terminal ring after the alkyne group. Each of the alkyne carbons has two orbitals with *sp* hybridisation and two non-hybrid p-orbitals, perpendicular to the *sp* orbitals and to each other. Consequently, one of these two non-hybrid p-orbitals is aligned with the non-hybrid p-orbital in the neighbouring carbons either side (which show *sp*² hybridisation). Thus the conjugated chain is expected to extend through the alkyne group to the double bond in the terminal ring. C=C bonds in end-rings are generally only partially conjugated, as steric hindrance causes the ring to rotate out of the plane³²⁻³³ – although this may not be the case for Ddx, in view of the absence of the hydrogen atom on carbon C7'. Depending on the precise

conformation of the end-ring, we therefore expect a theoretical N_{eff} between 9 and 10 for this carotenoid. In order to determine the exact N_{eff} , we measured the 0-0 electronic transition of Ddx in solvents of different polarizability (i.e. *n*-hexane, ethyl acetate, pyridine, and carbon disulfide). Figure 2 shows the absorption spectra exhibiting the three characteristic vibronic bands for monomer carotenoids in solution – note that these bands appear somewhat broader than simple linear carotenoids (supporting information, Fig. S5). The position of the 0-0 electronic transition of Ddx in each solvent is reported in Table 1 – the value in *n*-hexane (21035 cm^{-1}) is indeed between that of simple linear carotenoids spheroidene ($N=10$) and neurosporene ($N=9$) in *n*-hexane³⁰, consistent with an N_{eff} ca. 9.5.

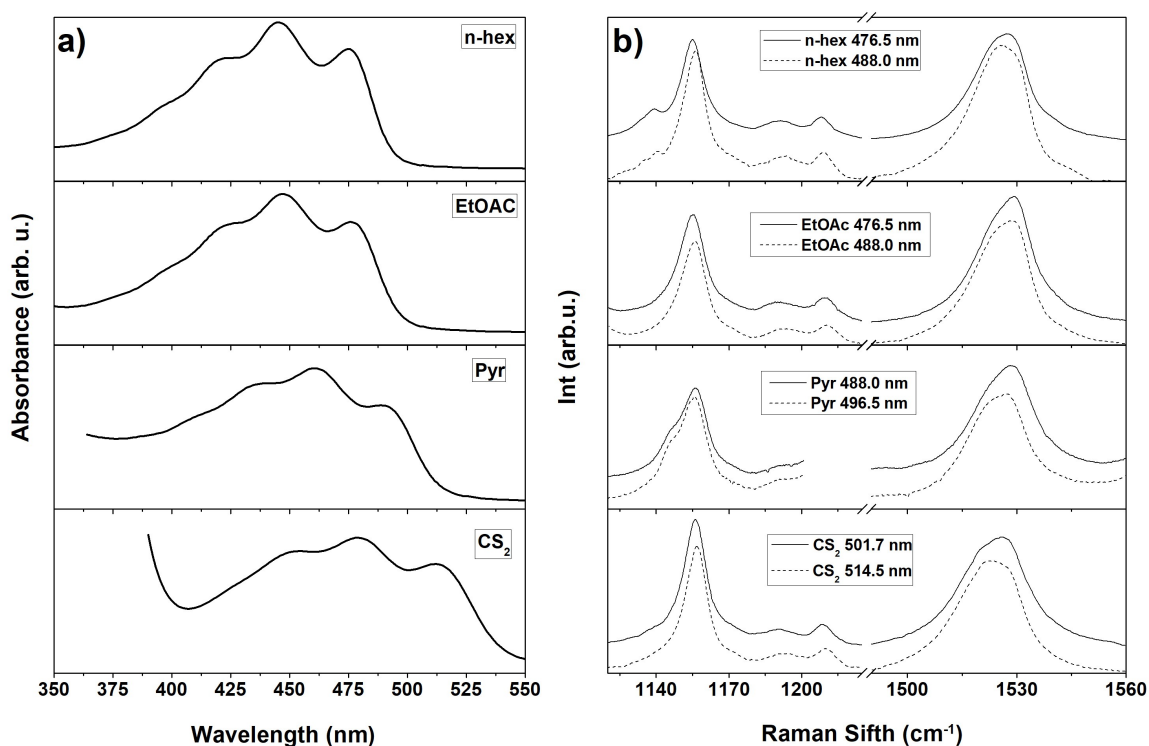


Figure 2/ Room temperature absorption (a) and resonance Raman (b) spectra of Diadinoxanthin in *n*-hexane, EtOAc, pyridine and CS_2 . Two resonance Raman excitations were used, both on the red side of the 0-0 electronic transition.

Resonance Raman, as a vibrational technique, yields direct information on the molecular properties of the carotenoid electronic ground state. The resonance Raman spectrum of carotenoids contains four main groups of bands, termed ν_1 to ν_4 ³⁹. The main ν_1 band arises from stretching modes of the conjugated C=C bonds, and gives access to the structure of the conjugated chain. Its

frequency is a direct measurement of the effective conjugation length of this chain, and it has been extensively used to characterise the properties of protein-bound carotenoid molecules²⁹. Simple carotenoids display a single Gaussian-like shape for this ν_1 band³⁰, whereas Ddx displays a double ν_1 peak at both excitation wavelengths, and in all solvents used (Figure 2b). We observe that both components of the ν_1 band downshift together toward lower energies as the polarizability of the solvent increases, as for the single-component ν_1 of “standard” carotenoids³⁰. Typically, the presence of more than one component in this spectral region is attributed to a mixed carotenoid population. However, additional purification steps, or isolation by a different protocol, still resulted in this apparently mixed population (data not shown), which thus does not result from the presence in the sample of another carotenoid species. Resonance Raman spectra recorded at two different excitation energies, both on the red side of the 0-0 transition, may be used to isolate individual carotenoids with shifted relative absorption within a mixed population, even when the mixture represents different conformers of the same carotenoid⁴⁰. The lower frequency component of the ν_1 band clearly gains intensity when shifting the excitation towards the red, revealing that this component arises from a Ddx conformation with a slightly red-shifted absorption. The ν_2 region, which arises from stretching vibrations of C-C single bonds coupled with C-H in-plane bending modes, constitutes a fingerprint for carotenoid C-C backbone isomerization (*cis/trans*)⁴¹⁻⁴³. For Ddx in all solvents, this region does not show any consistent sign of isomerization, which would be marked by a satellite band ca. 1130-1140 cm^{-1} appearing in the entire set of solvents. Hence, we can conclude that there is no isomerization in the main carotenoid C-C backbone, and Ddx is in the all-*trans* configuration.

Table 1/ Position of 0-0 transition and ν_1 component maxima for Ddx in *n*-hexane, Ethyl Acetate (EtOAc), Pyridine, and carbon disulphide (CS_2).

Ddx	0-0 transition	Excitation (nm)	ν_{1-1} (cm^{-1})	ν_{1-2} (cm^{-1})
<i>n</i>-Hexane	475.4 nm (21035 cm^{-1})	476.5	1523.2	1528.9
		488.0	1524.8	1529.3
EtOAc	476.5 nm (20986 cm^{-1})	476.5	1523.8	1529.3
		488.0	1523.5	1529.5
Pyridine	489.4 nm (20433 cm^{-1})	488.0	1522.1	1528.5
		496.5	1520.5	1527.6
CS_2	512.0 nm (19531 cm^{-1})	501.7	1519.8	1525.9
		514.5	1519.8	1525.9

Resonance Raman spectra of Ddx in pyridine were measured at low temperature (77 K) using a range of excitations across the 0-0 electronic transition (Figure 3). At low temperature, the doublet character of the ν_1 band disappears, resulting in a shape similar to that observed for regular carotenoids. However, the precise position of the ν_1 is highly excitation-dependent, gradually shifting from 1527.8 to 1532.6 cm^{-1} upon shifting the excitation from 488.0 to 514.5 nm. This is fully consistent with the mixture of Ddx conformations concluded from the experiments at room temperature. As the electronic transition narrows upon lowering the temperature, the resonance effect becomes more selective, and only one of the carotenoid conformers is observed in the resonance Raman spectra for each excitation. Hence, shifting the excitation results in the selective enhancement of different carotenoid species, inducing the observed shift in ν_1 band frequency.

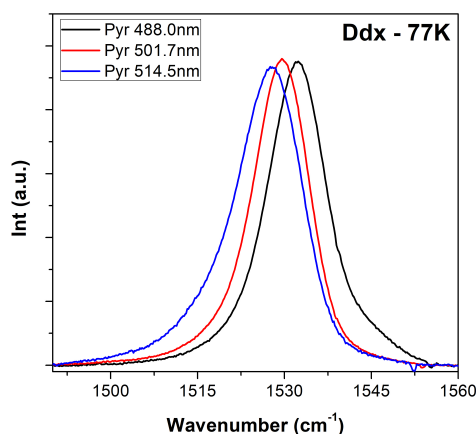


Figure 3/ Resonance Raman spectra in the ν_1 region of Ddx in pyridine at 77 K, for excitations at 488.0, 501.7 and 514.5 nm.

Electronic and Vibrational Properties of Alloxanthin.

We investigated alloxanthin (Allo) in order to determine whether the observed ν_1 doublet is specific for Ddx, or is rather a feature of alkyne carotenoids. Allo is a carotenoid with seven C=C double bonds and two alkyne groups in the linear chain, plus two conjugated terminal rings (Figure 1). The absorption spectra of Allo in solvents of different polarizability (*n*-hexane, EtOAc, Pyridine, and CS_2) are shown in Figure 4a; the values of the 0-0 transition for each solvent are reported in Table 2. The nominal conjugation length of Allo is 11, but the position of the 0-0 electronic transition of alloxanthin (20773 cm^{-1}) is at slightly higher energy than spheroidene (20644 cm^{-1}), indicating an effective conjugation length a little shorter than 10. The resonance Raman spectra of this alkyne carotenoid display the same features as Ddx – a splitting of the ν_1 at room temperature, where the

relative intensity of the two components is excitation-dependent. The positions of the ν_1 maxima are located at 1523 cm^{-1} and 1530 cm^{-1} in *n*-hexane, corresponding to effective conjugation lengths close to 10 and 9, respectively. As for Ddx, the $\Delta\nu_1$ between these two peaks for Allo seems to remain constant for all solvents used, within experimental error (± 0.5). The ν_2 region for Allo shows no sign of *cis* isomerization in any solvent, indicating that Allo is in the all-*trans* configuration. As both these carotenoid molecules display the same unusual ν_1 properties, we conclude that they are associated with the presence of the alkyne group in the conjugated C=C double bond chain. The doublet must be an intrinsic feature of alkyne carotenoids in solvents, and each of the ν_1 components corresponds to a different conformation with slightly different effective conjugation length. It was recently reported that the conformation of the conjugated end-cycles of β -carotene had an influence on the frequency of the Raman ν_1 band of this molecule³²⁻³³. It is therefore reasonable to consider whether the doublet has its origin in different conformations involving the conjugated end-ring(s).

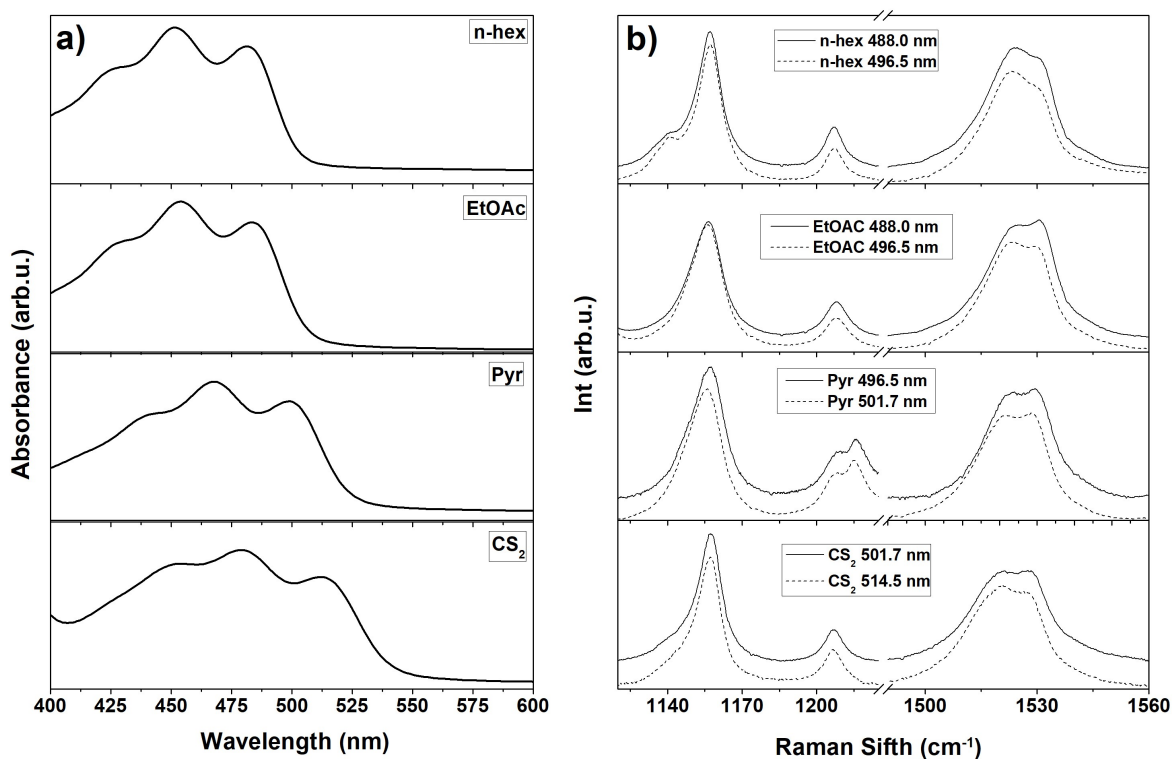


Figure 4/ Room temperature absorption (a) and resonance Raman (b) spectra of alloxanthin in *n*-hexane, EtOAc, pyridine and CS₂. Both Raman excitations were located on the red side of the 0-0 electronic transition.

Table 2/ Positions of 0-0 transition and ν_1 band components for Allo in n-hexane, ethyl acetate, pyridine and carbon disulphide at room temperature.

Allo	0-0 transition	Excitation (nm)	ν_{1-1} (cm^{-1})	ν_{1-2} (cm^{-1})
<i>n</i> -Hexane	481.4 nm (20773 cm^{-1})	488.0	1524.0	1530.7
		496.5	1523.4	1530.4
EtOAc	483.6 nm (20678 cm^{-1})	488.0	1524.4	1530.8
		496.5	1523.6	1529.8
Pyridine	498.9 nm (20044 cm^{-1})	496.5	1523.1	1529.5
		501.7	1522.8	1528.4
CS ₂	512.1 nm (19527 cm^{-1})	501.7	1520.3	1528.0
		514.5	1520.2	1527.5

Theoretical Modelling of Diadinoxanthin

In vacuo Calculations

We performed extensive simulations of Ddx in order to comprehend the physical origin of the uncommon ν_1 doublet in alkyne carotenoids. Only all-*trans* conformers were modelled, as the experimental data for Ddx showed no sign of *cis* isomerization for any solvent (no satellite bands ca. 1130-1140 cm^{-1} in Raman spectra; see above). We first simulated all-*trans* Ddx molecules *in vacuo* using the B3LYP/cc-pVDZ method^{31,44}. The complex electronic structure of carotenoids, with at least three lowest excited states with perturbed symmetries $1^1A_g^-$ (forbidden), $1^1B_u^-$ (forbidden) and $1^1B_u^+$ (strongly allowed) makes the calculation of the excited states somewhat complex. The determination of the lowest excited states can be predicted by involving the highest three occupied molecular orbitals (HOMO, HOMO-1, HOMO-2) and the lowest three unoccupied ones (LUMO, LUMO+1, and LUMO+2) in the calculation, as described elsewhere¹³⁻¹⁵. The B3LYP approach with CAM corrections yields a theoretical energy value for the $S_0 \rightarrow S_2$ transition of 2.6 eV (476.3 nm), and a resonance Raman spectrum containing a mono-modal ν_1 band similar to that usually observed for simple carotenoid molecules (1566.1 cm^{-1}). Hence, the mono-modal ν_1 band obtained in the calculations establishes that the alkyne group does not induce a combination of C=C modes leading to the experimentally-observed split of the ν_1 band. The ν_1 frequency is primarily sensitive to the structure of the C=C conjugated chain, which depends in part on the precise *cis/trans* configuration of the molecule. The experimental resonance Raman spectrum (Figure 2) reveals that Ddx is in an all-*trans* configuration, so a change in configuration of the C-C backbone is excluded as the origin of

the ν_1 doublet. However, it is possible that changes in the conformation of the conjugated end-cycle alter the effective conjugation length of Ddx. We searched for possible conformations of the Ddx molecule that could account for this split, analyzing the minimal conformation of the alkyne end-group of Ddx. As the triple bond is rigid, we studied in particular the conformation of the carbon atoms labelled $C10'-C9'-C6'-C5'$ (Figure 1) described by the dihedral angle (δ), which primarily represents the rotation angle around the C-C bonds either side of the triple bond. The two possible stable minima involving the end-cycle positions calculated *in vacuo* are shown in Figure 5a (see also supporting information, figure S1), $\delta = 183.15^\circ$ (*r-trans* type) and $\delta = 7.88^\circ$ (*r-cis* type).

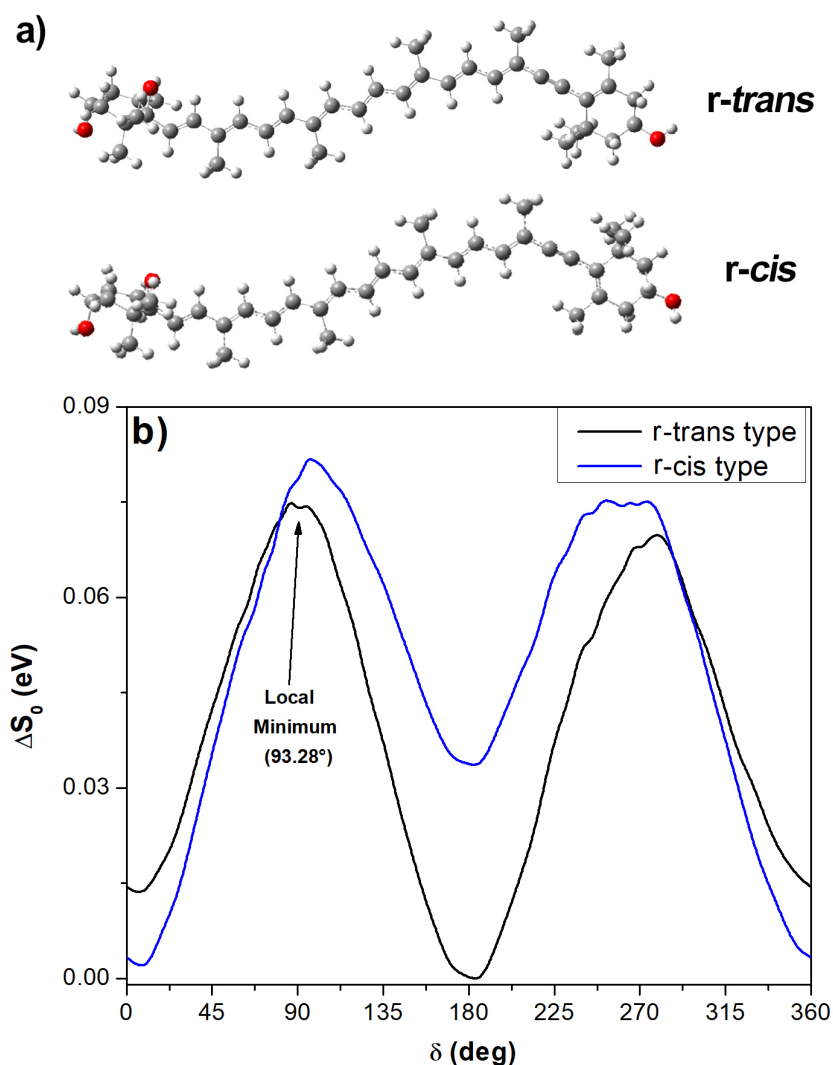


Figure 5/ a) The two minimized conformations for diadinoxanthin in vacuo, *r-trans* ($\delta = 183.15^\circ$) and *r-cis* ($\delta = 7.88^\circ$). **b)** The relative ground state energies according to end-group and polyene chain position, upon

rotation from the minimised starting conformations in **a**). δ is the dihedral angle between C10'-C9'-C6'-C5' (see Figure 1). The arrow marks an example of the many unstable local minima found in *vacuo*.

We took these two conformations as starting points to calculate the ground state energy of Ddx upon rotation of the dihedral angle (δ) between C10'-C9'-C6'-C5'. We observed two stable minima for δ values close to 180° (*r-trans* type) and 0° (*r-cis* type)(Figure 5b). These two values correspond to an in-plane position of the ring on one side of the triple bond relative to the polyene chain on the other, with an energy barrier for conversion between them lower than 0.1 eV. It is worth noting that this represents only ca. 30 % of the energy barrier calculated for standard carotenoids with conjugated end-cycles (e.g. β -carotene⁴⁵), implying that this isomerization can occur more easily for Ddx. The calculated C=C stretching frequency of Ddx in these two conformations is practically the same: 1566.1 cm⁻¹ (*r-trans* type) and 1566.2 cm⁻¹ (*r-cis* type). Hence, these conformations do not explain the ν_1 doublet observed experimentally. Interestingly, a number of local minima are observed, independently of the initial optimized molecular structure, in the 80°-100° and 270°-300° ranges of the dihedral angle (e.g. $\delta = 93.28^\circ$, indicated in Figure 5b). However, the vibrational and electronic properties of such *r-gauche*-type conformations³⁸ cannot be calculated, since they are unstable - evolving towards the *r-trans* or *r-cis* conformation upon minimization.

Simulations in the presence of solvent

The untestable conformation(s) of the alkyne group observed *in vacuo* represents a potential candidate to explain the experimental properties of Ddx. To attempt to stabilize these local minima, we first performed polarizable continuum model (PCM) simulations in different solvents. These calculations in acetonitrile, *n*-hexane and pyridine gave similar results to those obtained *in vacuo* (data not shown). They reveal the presence of several dihedral angle conformations with local minima in the 80°-100° and 270°-300° ranges of the dihedral angle, but they were unstable and evolved toward the two global minima (*r-cis* or *r-trans* conformation). We therefore attempted a supermolecular approach, to stabilize the structures at their local minima using hydrogen bonds from water molecules³⁷. We generated a Ddx molecule in one of these *r-gauche* conformations ($\delta = 93.28^\circ$), and solvated it with 139 water molecules using the PACKMOL package⁴⁶. We then performed Car-Parrinello molecular dynamics (QMD) on this ensemble, and obtained the time-dependent evolution of the dihedral δ angle at 300 K (Figure 6). This angle presents fluctuations around 90° over the 1.5 ps timescale of the simulation, confirming that the 139 water molecules are

indeed able to stabilize this *r-gauche* conformation – δ remains within the range 80-110°, rather than evolving towards 0/180°.

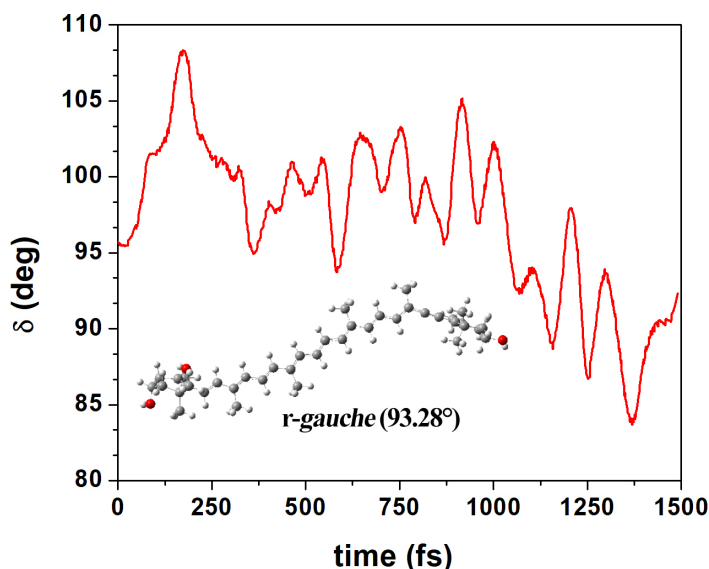


Figure 6/ Collected data for static modelling: temporal evolution of the δ dihedral angle of Diadinoxanthin surrounded by 139 water molecules; Car-Parrinello MD calculations at 300 K. **Inset:** Stable minimum with the conjugated end-ring in *r-gauche* conformation.

To determine the minimum number of water molecules required to stabilize the *r-gauche* conformation, we first removed those waters not immediately surrounding the alkyne-side terminal ring, keeping 29 water molecules solvating both sides of this ring and 2 water molecules in the opposite non-conjugated ring. This ensemble (*r-gauche* Ddx + 31 HOH) was then optimized by DFT, confirming that the *r-gauche* conformation remained stable (Supporting Information, Figure S2). We then further reduced the number of water molecules progressively, first on side A and then on side B of the ring (see Figure 1). In each case, the ensemble structure was minimized and the stabilized *r-gauche* conformation was then used to calculate the dihedral angle and the ν_1 band position (Supporting Information, Table S1). All structures with characteristic imaginary frequencies, and those which reverted to the *r-cis* or *r-trans* structures as a result of the optimization procedure, were excluded from the analysis. During the optimization procedure of the Ddx structure the water molecules were fixed as defined from QMD calculations. This process led to a number of *r-gauche* structures stabilized by only a few water molecules – an example of such an ensemble, with only

five solvating water molecules on side B and $\delta = 90.35^\circ$, is given in Supporting Information, Figure S2.

Stabilizing the *r-gauche* conformation with a minimal number of water molecules then allowed us to calculate the electronic and vibrational properties of this conformer, and compare them with the properties of the *r-trans* (183.18°) and *r-cis* (7.88°) conformers *in vacuo* (see above). For each structure, we determined the molecular orbitals involved in the $S_0 \rightarrow S_2$ transition: HOMO, HOMO-1, HOMO-2, LUMO, LUMO+1, and LUMO+2 (Supplementary Information, Figure S3). These π -orbitals are localized principally on the polyene chain, but extend to the ring C=C, for the *r-trans* and *r-cis* conformers - as observed previously for carotenoids with conjugated terminal rings^{13, 31}. On the other hand, the *r-gauche* conformer exhibits remarkably different HOMO-2 and LUMO+2 π -orbitals, involving the end-ring and only extending up to the triple bond (Figure 7). The HOMO, HOMO-1, LUMO and LUMO+1 orbitals also exhibit differences from the *cis* and *trans* conformations, extending the length of the polyene chain but ending at the alkyne group (Supplementary Information, Figure S2). Hence, the electronic and vibrational properties of this conformer may be significantly different, since the HOMO-2 and LUMO+2 orbitals have significant influence on these properties. We calculated the six molecular orbitals for several of the *r-gauche* conformers, where the water molecules were at different positions (Supplementary Information, Table S1). The Raman ν_1 frequencies calculated for each of the *r-gauche* structures are ca. 1570 cm^{-1} - around 6 cm^{-1} higher than that observed for the global minima *in vacuo* (*r-cis* or *r-trans*, $0/180^\circ$). The calculated pairs of values ($S_0 \rightarrow S_2$ and ν_1) for each *r-gauche* Ddx conformer according to δ angle value and number of water molecules is reported in Table 3. It is worth noting that, as each of the calculated structures are surrounded by water molecules at different positions, and the $S_0 \rightarrow S_2$ state is sensitive to the presence of solvent, the calculated values are merely indicative of the tendencies in these shifts. The largest calculated difference between planar and *r-gauche*-type conformers of Ddx is 16 nm, but this may vary depending on the nature of the solvent used for stabilization.

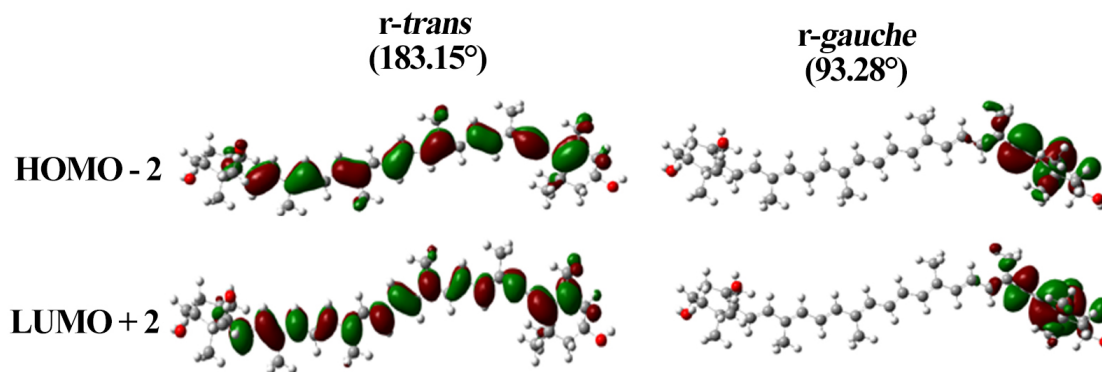


Figure 7/ Molecular orbitals presenting significant changes, HOMO-2 and LUMO+2, for diadinoxanthin in conformations *r-trans* (in vacuo) and *r-gauche* (stabilized by five waters). The entire ensemble of molecular orbitals are in supporting information, Figure S2.

Table 3/ Calculated position of $S_0 \rightarrow S_2$ and ν_1 according to δ dihedral angle, for *r-gauche* Ddx stabilised by water molecules.

Water molecules	δ (deg)	$S_0 \rightarrow S_2$ (nm)*	ν_1 frequency (cm^{-1})
0**	183.18	476.26	1566.09
4	180.74	477.13	1565.91
5	74.82	462.41	1571.24
5	78.91	460.87	1571.81
5	83.23	460.53	1571.83
5	90.35	460.52	1571.76

* CAM functional corrections involved in calculations

** in vacuo

Discussion and Conclusions

In this paper, we have designed a strategy for calculating the spectroscopic properties of complex, conjugated molecules in non-minimum conformations, and have applied this strategy to account for the properties of alkyne carotenoids in solvents. These carotenoids (diadinoxanthin and alloxanthin) both exhibit an effective conjugation length shorter than that deduced from their structure, and resonance Raman spectra exhibit an abnormal split ν_1 band. DFT calculations, performed on diadinoxanthin minimized structures, suggest that the presence of the alkyne group does not induce any large redistribution in the C=C stretching modes that could explain the observed

ν_1 splitting. The relative contributions of the two ν_1 components vary according to the excitation conditions, suggesting the presence of populations with slightly shifted absorption transitions in all solvents studied. At low temperature, the ν_1 band becomes sharper and highly excitation-dependent, again suggesting the presence of different conformations of these molecules with slightly shifted absorption maxima. We concluded that mixtures of alkyne carotenoid conformations occur in solvents - we therefore set out to model these conformations.

The energy calculations performed *in vacuo* on diadinoxanthin suggest that this carotenoid may present conformations with values of the δ dihedral angle of the end-ring close to $0/180^\circ$ (flat positions) and $90/270^\circ$ (perpendicular positions). The Ddx conformation corresponding to $\delta=90^\circ$ was not stable *in vacuo* during minimization, rendering calculation of its electronic and vibrational properties impossible. The ground state energies of carotenoids may differ considerably in vacuum and in solvents, due to the presence of heteroatoms. We therefore performed Polarizable continuum model (PCM) calculations on diadinoxanthin solvated by water, pyridine, acetonitrile and n-hexane molecules. PCM optimization of the *r-gauche* structure could not be achieved in any solvent – with the exception of water (see below) – since the barriers separating the relevant local *r-gauche* minima were very small (see Fig. 5 and Supporting Information Fig. S4). Water is not an ideal solvent for hydrophobic molecules, but it exhibits a marked ability to form hydrogen bonds – which may interact with the molecule in such a way as to stabilize new conformations. Car-Parinello molecular dynamics allowed the determination of an *r-gauche* conformation stabilized by waters, which was then progressively desolvated. As a result, we obtained Ddx accompanied by a small number of water molecules in *r-gauche* conformations with slightly different values of the dihedral angle. These conformations were stable enough to allow an extensive set of DFT calculations to be performed, allowing us to model the changes in electronic and vibrational properties of diadinoxanthin according to δ . Calculation of the orbitals of *r-gauche* Ddx generated HOMO-2 and LUMO+2 orbitals located on the end grouping involving the alkyne bond (Supplementary Information, Figure S3), whereas they are expected along the conjugated chain (see other orbitals in Fig S3). Thus where high-accuracy quantum chemistry calculations are required, such as EOM-CCSD, CASSCF or SAC-CI, these should be applied with larger orbital windows or with differentially-reorganized π -orbitals for the *r-gauche* Ddx case. To apply the simplest semi-empirical method, we use 6 orbital windows to predict the perturbed symmetry states $1^1A_g^-$ and $1^1B_u^-$.¹³ Some carotenoids

in solvents exhibit so-called intra-molecular charge transfer (ICT) states⁴⁷. However, these do not appear in our calculations, suggesting that ICT states are not present in Ddx conformers.

The ν_1 band splitting observed experimentally is consistently larger for Allo than for Ddx molecules (see Table 1 and Table 2). As follows from our model calculations, this splitting value should strongly depend on the angle between the polyene chain and the end-ring (Supplementary Information, Table S1), as a result of different stabilization of the structure by solvent molecules. The QMD (Figure 6) may be a good tool for searching the relevant structures in different local minima for longer times, in order to fine-tune these angles in future calculations on other systems. Experimentally, Ddx in *n*-hexane exhibits the $S_0 \rightarrow S_2$ transition at 475.4 nm and ν_1 values at 1523.2 and 1528.9 cm^{-1} . Using the CAM-B3LYP/cc-pVDZ calculation level for *r-gauche* (five waters) and *r-cis* (*in vacuo*), the values obtained were (460.5 nm, 1571.4 cm^{-1}) and (477.1 nm, 1565.9 cm^{-1}), respectively. The results show that the *r-gauche* conformation of the terminal ring has a direct effect on the frequency of the ν_1 C=C stretching band, upshifting it by 6 cm^{-1} . The calculations also describe the effect the *r-gauche* conformation has on the $S_0 \rightarrow S_2$ transition consistently, with a calculated downshift of 10-16 nm relative to *r-cis*. The absorption spectra recorded for Ddx and Allo in different solvents do not present any obvious features indicating the presence of different conformers. We simulated the absorption spectra of such mixtures, for several ratios of all-*trans* lycopene and red-shifted all-*trans* lycopene – the latter red-shifted by 15 nm, as estimated for a ν_1 difference of 5 cm^{-1} (Supporting Information, Figure S5)³⁰. These linear combinations produce absorption spectra with barely distorted features up to 8:2 mixtures, although the peaks are significantly broader - as observed experimentally for Ddx and Allo (Fig. 2a). This suggests that the presence of an additional conformer at this molar ratio or less cannot be distinguished in the absorption spectrum.

On this basis, we can explain the ensemble of Ddx properties by proposing that the conjugated end-ring of alkyne carotenoids in solution explores a third meta-stable conformation (in addition to the two stable, planar ones). It is of note that the QMD calculations which led to this result were performed in water, which is not a natural solvent for Ddx. This choice was driven purely by the notion, supported by the Car-Parinello MD, that the hydrogen bonding properties of water could stabilize a non-global minimum conformation sufficiently to allow this supermolecular modelling approach. To our knowledge, this is the first time that a carotenoid in a distorted conformation could be successfully modelled. It shows in particular the spectacular effect of the distortion on the molecular orbitals of the carotenoid. Predicting the properties of molecules out of their minimal

conformation is a general pitfall in modelling studies, and this approach should have wide-ranging applications for QMD calculations on such distorted conformers.

Materials and Methods

Pigment purification

Diadinoxanthin was purified from cells of the marine diatom *Phaeodactylum tricornutum* (SAG collection, strain 1090-1a). Alloxanthin was purified from cells of the marine cryptophyte *Rhodomonas salina* (strain CCAP 978/27)⁴⁸. Sample preparation was performed in the dark, on ice. Cells were separated from the culture medium by centrifugation (7000×g, 5 min), and the pigments extracted in three solubilisation steps - in methanol twice, and finally acetone. In each step, the pellet was suspended in the solvent and sonicated to induce pigment release. The cell material was then removed by centrifugation (13000×g, 1 min), to be used in the following step. The cell material remained colorless after the third step. The extracts were then pooled and dried under vacuum before dissolving in methanol prior to purification. The pigments were purified using an HPLC system consisting of a Pump Controller Delta 600, a manual injection system and a PDA 2996 detector (Waters, USA). The pigments were separated on a reverse-phase Zorbax SB-C18 column (4.6 × 150 mm, 5 μm, silica-based, non-encapped; Agilent, USA), using a linear elution gradient at a 1 ml min⁻¹ flow rate. A ternary solvent system was used as follows: 0 - 4 min linear gradient from 100 % Solvent-A to 100 % Solvent-B, 4 - 18 min linear gradient from 100 % B to 20 % B / 80% C. (Solvent-A - 80:20 methanol:0.5 M ammonium acetate (aq., pH 7.2 v/v); Solvent-B - 90:10 acetonitrile:water; Solvent-C - 100 % ethyl acetate)⁴⁹. The pigments were identified based on their absorption spectra and retention times. The peaks of interest were collected, dried out in the dark under vacuum and stored at -80°C. The purity of the final pigment preparation was verified by HPLC using the same protocol⁴⁹.

UV-Vis Absorption. Absorption spectra were measured using a Varian Cary E5 Double-beam scanning spectrophotometer with a 1.0 cm path length cuvette.

Resonance Raman spectra were recorded at room temperature and 77 K, the latter with an LN2-flow cryostat (Air Liquide, France). Laser excitations at 476.5, 488.0, 501.7 & 514.5 nm were obtained with an Ar⁺ Sabre laser (Coherent). Output laser powers of 10–100 mW were attenuated

to < 5 mW at the sample. Scattered light was focused into a Jobin-Yvon U1000 double-grating spectrometer (1800 grooves/mm gratings) equipped with a red-sensitive, back-illuminated, LN₂-cooled CCD camera. Sample stability and integrity were assessed based on the similarity between the first and last Raman spectra.

Static calculations

The B3LYP functional in combination with the 6-311G(d,p) and cc-pVDZ basis set is known to provide reasonably good geometries^{4, 31}. DFT-based methods are able to perform calculations of the vibrational frequency with an overall root mean square error of 34–48 cm⁻¹, significantly less than that reported for MP2 theory (61 cm⁻¹)⁵. A scaling factor of 0.96 is used for frequencies calculated by the B3LYP/6-31G(d) method, in order to obtain reasonable agreement with the experimental data^{5, 31, 44}. A polar environment can cause the shift of Raman frequencies³¹, which can be determined for specific solvents by the PCM method, with a proportional shift between experiment and calculations^{6, 31, 37}. We chose the B3LYP/cc-pVDZ method for the present study, available in the Gaussian 09 package (Rev D.01)⁵⁰. The calculations were performed with the “nosymm” keyword, disabling attempts to identify the point group of the molecule. The end-group energy surfaces were calculated by changing the dihedral angle artificially from 0 to 360 deg in 0.5 deg steps, and calculating the ground state energy. The stabilized conformations obtained after Car-Parinello Molecular Dynamics were used for geometry optimization, and determination of energetic levels and Raman frequencies.

Molecular dynamics calculations

Car-Parinello Molecular Dynamics (QMD) calculations were carried out using the NwChem program ver 6.6⁵¹, with the initial molecular Ddx conformer in the gas phase optimized by DFT methods. Taking this conformer as starting structure, we rotated the end-group by 90 degs and obtained the initial conformations for Molecular Dynamics Simulations. Water molecules were added using PACKMOL⁴⁶, locating the packed molecules (Ddx and 139 water molecules) in a simple 40 Å x 40 Å x 40 Å cube. Car-Parrinello molecular dynamics were carried out at 300 K with a time step of 3.0 a.u. (0.07257 fs), coupled to a Nosé-Hoovwe chains thermostat¹ at a frequency of 1200 cm⁻¹. An electronic mass parameter of 450 a.u. was implemented. Electronic exchange and correlation were modeled using the gradient-corrected functional of Perdew, Burke and Ernzerhof (PBE)². Core electrons were treated using the norm-conserving atomic pseudopotentials (PP) of

Troullier and Martins³, while valence electrons were represented in a planewave basis set truncated at an extended energy cut-off of 20 Ry. Following the initial equilibration period, data was accrued further (1.5 ps) for the Car-Parrinello dynamics on the parent model. The data were analyzed and visualized using the Chemcraft 1.6⁵², GaussView 5.0⁵⁰ and VMD 1.9.2⁵³ programs.

Supporting Information

A supporting information file is available with the molecular structures of *r-trans* and *r-cis* diadinoxanthin. The HOMO orbital of diadinoxanthin stabilized with 31 water molecules. The molecular orbitals HOMO, HOMO-1, HOMO-2, LUMO, LUMO+1 and LUMO+2, in diadinoxanthin *r-trans* & *r-cis* configurations (in vacuo), and *r-gauche* configuration stabilized by five water molecules. The relative ground state energies according to end-group and polyene chain position, upon rotation from the minimised starting conformations in diadinoxanthin. A simulation of the absorption spectra of a mixture of carotenoids with different conjugation length, using lycopene in *n*-hexane as reference. The HPLC chromatograms of purified pigments prior to the spectroscopic experiments. A table showing Raman ν_1 frequency correlations with the δ angle position of Ddx. The structure of diadinoxanthin in configuration *r-gauche* (93.28°). XYZ structure at b3lyp/cc-pVDZ calculation level.

Acknowledgments

Spectroscopic measurements were performed on the Biophysics Platform of I2BC; computations on resources at the High Performance Computing Center “HPC Sauletekis” in Vilnius University Faculty of Physics. The skilled technical assistance of Frantisek Matousek in purification of carotenoids is gratefully acknowledged. This work was supported by the ERC funding agency (PHOTPROT project), the French Infrastructure for Integrated Structural Biology (FRISBI) ANR-10-INBS-05, the European Union’s Horizon 2020 research and innovation program under the Marie Skłodowska-Curie grant agreement No 675006 (SE2B), and Gilibert project S-LZ-19-3. The work in the Czech Republic was supported by the Czech Science Foundation projects 19-11494S (E. Kuthanová Trsková) and 31-19-28323X (R. Litvin). Institutional support RVO:60077344 and Institutional project Algatech Plus (MSMT LO1416) of the Czech Ministry of Education, Youth and Sport are also acknowledged.

References

1. Martyna, G. J.; Klein, M. L., Nosé–Hoover chains: The canonical ensemble via continuous dynamics. *J. Chem. Phys.* **1992**, *97* (4), 2635-2643.
2. Perdew, J. P.; Burke, K.; Ernzerhof, M., Generalized Gradient Approximation Made Simple. *Phys. Rev. Lett.* **1996**, *77* (18), 3865-3868.
3. Troullier, N.; Martins, J. L., Efficient pseudopotentials for plane-wave calculations. *Physical Review B* **1991**, *43* (3), 1993-2006.
4. Dreuw, A.; Harbach, P. H. P.; Mewes, J. M.; Wormit, M., Quantum chemical excited state calculations on pigment–protein complexes require thorough geometry re-optimization of experimental crystal structures. *Theor. Chem. Acc.* **2010**, *125* (3), 419-426.
5. Wong, M. W., Vibrational frequency prediction using density functional theory. *Chem. Phys. Lett.* **1996**, *256* (4), 391-399.
6. Liu, W.; Wang, Z.; Zheng, Z.; Jiang, L.; Yang, Y.; Zhao, L.; Su, W., Density Functional Theoretical Analysis of the Molecular Structural Effects on Raman Spectra of β -Carotene and Lycopene. *Chin. J. Chem.* **2012**, *30* (10), 2573-2580.
7. Mardirossian, N.; Head-Gordon, M., Thirty years of density functional theory in computational chemistry: an overview and extensive assessment of 200 density functionals. *Mol. Phys.* **2017**, *115* (19), 2315-2372.
8. Cohen, A. J.; Mori-Sánchez, P.; Yang, W., Challenges for Density Functional Theory. *Chem. Rev. (Washington, DC, U. S.)* **2012**, *112* (1), 289-320.
9. Chung, L. W.; Sameera, W. M. C.; Ramezani, R.; Page, A. J.; Hatanaka, M.; Petrova, G. P.; Harris, T. V.; Li, X.; Ke, Z.; Liu, F.; Li, H.-B.; Ding, L.; Morokuma, K., The ONIOM Method and Its Applications. *Chem. Rev. (Washington, DC, U. S.)* **2015**, *115* (12), 5678-5796.
10. Hutter, J., Car–Parrinello molecular dynamics. *Wiley Interdisciplinary Reviews: Computational Molecular Science* **2012**, *2* (4), 604-612.
11. Kühne, T. D., Second generation Car–Parrinello molecular dynamics. *Wiley Interdisciplinary Reviews: Computational Molecular Science* **2014**, *4* (4), 391-406.
12. Rudberg, E.; Sałek, P.; Helgaker, T.; Ågren, H., Calculations of two-photon charge-transfer excitations using Coulomb-attenuated density-functional theory. *J. Chem. Phys.* **2005**, *123* (18), 184108.
13. Macernis, M.; Sulskus, J.; Duffy, C. D. P.; Ruban, A. V.; Valkunas, L., Electronic Spectra of Structurally Deformed Lutein. *J. Phys. Chem. A* **2012**, *116* (40), 9843-9853.
14. Cunningham, F. X., Jr.; Gantt, E., One ring or two? Determination of ring number in carotenoids by lycopene epsilon-cyclases. *Proceedings of the National Academy of Sciences of the United States of America* **2001**, *98* (5), 2905-2910.
15. Tschirner, N.; Schenderlein, M.; Brose, K.; Schlodder, E.; Mroginiski, M. A.; Hildebrandt, P.; Thomsen, C., Raman excitation profiles of β -carotene – novel insights into the nature of the v1-band. *physica status solidi (b)* **2008**, *245* (10), 2225-2228.

16. Britton, G.; Liaaen-Jensen, S.; Pfander, H., *Carotenoids, Volume 4: Natural Functions*. Birkhäuser Verlag: Switzerland, 2008.
17. Frank, H. A.; Young, A. J.; Britton, G.; Cogdell, R. J., *The Photochemistry of Carotenoids*. Kluwer Academic Publishing: 1999.
18. Thomas, D. B.; McGraw, K. J.; Butler, M. W.; Carrano, M. T.; Madden, O.; James, H. F., Ancient origins and multiple appearances of carotenoid-pigmented feathers in birds. *Proceedings of the Royal Society B: Biological Sciences* **2014**, *281* (1788), 20140806.
19. Zhao, C.; Nability, P. D., Phylloxerids share ancestral carotenoid biosynthesis genes of fungal origin with aphids and adelgids. *PLoS One* **2017**, *12* (10), e0185484.
20. Harrison, E. H.; Quadro, L., Apocarotenoids: Emerging Roles in Mammals. *Annu. Rev. Nutr.* **2018**, *38* (1), 153-172.
21. Saint, S. E.; Renzi-Hammond, L. M.; Khan, N. A. H., C.H.; Frick, J. E. H., B.R. , The Macular Carotenoids are Associated with Cognitive Function in Preadolescent Children. *Nutrients* **2018**, *10*, 193.
22. Hou, X.; Rivers, J.; León, P.; McQuinn, R. P.; Pogson, B. J., Synthesis and Function of Apocarotenoid Signals in Plants. *Trends Plant Sci.* **2016**, *21* (9), 792-803.
23. Tavan, P.; Schulten, K., Electronic excitations in finite and infinite polyenes. *Physical Review B* **1987**, *36* (8), 4337-4358.
24. Polívka, T.; Sundström, V., Ultrafast Dynamics of Carotenoid Excited States—From Solution to Natural and Artificial Systems. *Chem. Rev. (Washington, DC, U. S.)* **2004**, *104* (4), 2021-2072.
25. Schulten, K.; Karplus, M., On the origin of a low-lying forbidden transition in polyenes and related molecules. *Chem. Phys. Lett.* **1972**, *14* (3), 305-309.
26. Frank, H. A., Spectroscopic Studies of the Low-Lying Singlet Excited Electronic States and Photochemical Properties of Carotenoids. *Arch. Biochem. Biophys.* **2001**, *385* (1), 53-60.
27. Rondonuwu, F. S.; Yokoyama, K.; Fujii, R.; Koyama, Y.; Cogdell, R. J.; Watanabe, Y., The role of the $1B_u^-$ state in carotenoid-to-bacteriochlorophyll singlet-energy transfer in the LH2 antenna complexes from *Rhodobacter sphaeroides* G1C, *Rhodobacter sphaeroides* 2.4.1, *Rhodospirillum molischianum* and *Rhodopseudomonas acidophila*. *Chem. Phys. Lett.* **2004**, *390* (4), 314-322.
28. Nishimura, K.; Rondonuwu, F. S.; Fujii, R.; Akahane, J.; Koyama, Y.; Kobayashi, T., Sequential singlet internal conversion of $1B_u^+ \rightarrow 3A_g^- \rightarrow 1B_u^- \rightarrow 2A_g^- \rightarrow (1A_g^- \text{ ground})$ in all-trans-spirilloxanthin revealed by two-dimensional sub-5-fs spectroscopy. *Chem. Phys. Lett.* **2004**, *392* (1), 68-73.
29. Llansola-Portoles, M. J.; Pascal, A. A.; Robert, B., Electronic and vibrational properties of carotenoids: from in vitro to in vivo. *Journal of The Royal Society Interface* **2017**, *14* (135).
30. Mendes-Pinto, M. M.; Sansiaume, E.; Hashimoto, H.; Pascal, A. A.; Gall, A.; Robert, B., Electronic Absorption and Ground State Structure of Carotenoid Molecules. *J. Phys. Chem. B* **2013**, *117* (38), 11015-11021.
31. Macernis, M.; Sulskus, J.; Malickaja, S.; Robert, B.; Valkunas, L., Resonance Raman Spectra and Electronic Transitions in Carotenoids: A Density Functional Theory Study. *J. Phys. Chem. A* **2014**, *118* (10), 1817-1825.

32. Mendes-Pinto, M. M.; Galzerano, D.; Telfer, A.; Pascal, A. A.; Robert, B.; Ilioaia, C., Mechanisms Underlying Carotenoid Absorption in Oxygenic Photosynthetic Proteins. *J. Biol. Chem.* **2013**, *288* (26), 18758-18765.
33. Llansola-Portoles, M. J.; Sobotka, R.; Kish, E.; Shukla, M. K.; Pascal, A. A.; Polívka, T.; Robert, B., Twisting a β -Carotene, an Adaptive Trick from Nature for Dissipating Energy during Photoprotection. *J. Biol. Chem.* **2017**, *292* (4), 1396-1403.
34. Kaňa, R.; Kotabová, E.; Sobotka, R.; Prášil, O., Non-Photochemical Quenching in Cryptophyte Alga *Rhodomonas salina* Is Located in Chlorophyll a/c Antennae. *PLoS One* **2012**, *7* (1), e29700.
35. Streckaite, S.; Gardian, Z.; Li, F.; Pascal, A. A.; Litvin, R.; Robert, B.; Llansola-Portoles, M. J., Pigment configuration in the light-harvesting Protein of the Xanthophyte alga *Xanthonema debile*. *Photosynth. Res.* **2018**, *138* (1), 139-148.
36. Goss, R.; Jakob, T., Regulation and function of xanthophyll cycle-dependent photoprotection in algae. *Photosynth. Res.* **2010**, *106* (1-2), 103-122.
37. Macernis, M.; Kietis, B. P.; Sulskus, J.; Lin, S. H.; Hayashi, M.; Valkunas, L., Triggering the proton transfer by H-bond network. *Chem. Phys. Lett.* **2008**, *466* (4), 223-226.
38. Moss, G. P., Basic terminology of stereochemistry (IUPAC Recommendations 1996). In *Pure Appl. Chem.*, 1996; Vol. 68, p 2193.
39. Gill, D.; Kilponen, R. G.; Rimai, L., Resonance Raman Scattering of Laser Radiation by Vibrational Modes of Carotenoid Pigment Molecules in Intact Plant Tissues. *Nature* **1970**, *227* (5259), 743-744.
40. Ruban, A. V.; Pascal, A. A.; Robert, B., Xanthophylls of the major photosynthetic light-harvesting complex of plants: identification, conformation and dynamics. *FEBS Lett.* **2000**, *477* (3), 181-185.
41. Koyama, Y.; Takatsuka, I.; Nakata, M.; Tasumi, M., Raman and infrared spectra of the all-trans, 7-cis, 9-cis, 13-cis and 15-cis isomers of β -carotene: Key bands distinguishing stretched or terminal-bent configurations from central-bent configurations. *J. Raman Spectrosc.* **1988**, *19* (1), 37-49.
42. Koyama, Y.; Takii, T.; Saiki, K.; Tsukida, K., Configuration of the carotenoid in the reaction centers of photosynthetic bacteria. 2. Comparison of the resonance Raman lines of the reaction centers with those of the 14 different cis-trans isomers of β -carotene. *Photobiophys. Photobiophys.* **1983**, *5*, 139-150.
43. Koyama, Y.; Kito, M.; Takii, T.; Saiki, K.; Tsukida, K.; Yamashita, J., Configuration of the carotenoid in the reaction centers of photosynthetic bacteria. Comparison of the resonance Raman spectrum of the reaction center of *Rhodospseudomonas sphaeroides* G1C with those of cis-trans isomers of β -carotene. *Biochim. Biophys. Acta, Bioenerg.* **1982**, *680* (2), 109-118.
44. Macernis, M.; Galzerano, D.; Sulskus, J.; Kish, E.; Kim, Y.-H.; Koo, S.; Valkunas, L.; Robert, B., Resonance Raman Spectra of Carotenoid Molecules: Influence of Methyl Substitutions. *J. Phys. Chem. A* **2015**, *119* (1), 56-66.
45. Liu, W.-L.; Wang, Z.-G.; Zheng, Z.-R.; Li, A.-H.; Su, W.-H., Effect of β -Ring Rotation on the Structures and Vibrational Spectra of β -Carotene: Density Functional Theory Analysis. *J. Phys. Chem. A* **2008**, *112* (42), 10580-10585.
46. Martínez, L.; Andrade, R.; Birgin, E. G.; Martínez, J. M., PACKMOL: A package for building initial configurations for molecular dynamics simulations. *J. Comput. Chem.* **2009**, *30* (13), 2157-2164.

47. Redeckas, K.; Voiciuk, V.; Vengris, M., Investigation of the S1/ICT equilibrium in fucoxanthin by ultrafast pump-dump-probe and femtosecond stimulated Raman scattering spectroscopy. *Photosynth. Res.* **2016**, *128* (2), 169-181.
48. West, R.; Keřan, G.; Trsková, E.; Sobotka, R.; Kařa, R.; Fuciman, M.; Polívka, T., Spectroscopic properties of the triple bond carotenoid alloxanthin. *Chem. Phys. Lett.* **2016**, *653*, 167-172.
49. Llansola-Portoles, M. J.; Uragami, C.; Pascal, A. A.; Bina, D.; Litvin, R.; Robert, B., Pigment structure in the FCP-like light-harvesting complex from *Chromera velia*. *Biochim. Biophys. Acta, Bioenerg.* **2016**, *1857* (11), 1759-1765.
50. Frisch, M. J.; Trucks, G. W.; Schlegel, H. B.; Scuseria, G. E.; Robb, M. A.; Cheeseman, J. R.; Scalmani, G.; Barone, V.; Mennucci, B.; Petersson, G. A. e. a., . Gaussian 09. Gaussian, Inc.: Wallingford, CT, USA, 2009.
51. Valiev, M.; Bylaska, E. J.; Govind, N.; Kowalski, K.; Straatsma, T. P.; Van Dam, H. J. J.; Wang, D.; Nieplocha, J.; Apra, E.; Windus, T. L.; de Jong, W. A., NWChem: A comprehensive and scalable open-source solution for large scale molecular simulations. *Comput. Phys. Commun.* **2010**, *181* (9), 1477-1489.
52. Chemcraft *Graphical software for visualization of quantum chemistry computations.* <https://www.chemcraftprog.com>.
53. Humphrey, W.; Dalke, A.; Schulten, K., VMD: Visual molecular dynamics. *Journal of Molecular Graphics* **1996**, *14* (1), 33-38.